J Fluoresc (2009) 19:631–639
DOI 10.1007/s10895-008-0454-7

ORIGINAL PAPER

Steady-State and Time-Resolved Fluorescence Spectroscopic Studies on Interaction of the N-terminal Region with the Hairpin Loop of the Phytocystain Scb

Keiko Doi-Kawano · Etsuko Nishimoto · Yoshiaki Kouzuma · Daisuke Takahashi · Shoji Yamashita · Makoto Kimura

Received: 22 November 2007 / Accepted: 9 December 2008 / Published online: 23 December 2008

Abstract The steady-state and time-resolved fluorescece spectroscopy is one of the most powerful method to detect and analyze subtle conformation change and interaction between peptide elements in protein. Phytocystatin Scb isolated from sunflower seeds includes a single Trp residue at position 85. In an attempt to investigate the interaction of the N-terminal region of Scb with the first and second hairpin loops by fluorescence spectroscopy of Trp residue, two Scb mutants in which single Trp locates at position 52 and 58, respectively, and their N-terminal removed mutants were generated. The N-terminal truncation changed the fluorescence decay kinetics of Trp52 from the triple exponential to double. Furthermore, the time-resolved fluorescence anisotropy residue indicated that the segmental motion of Trp52 was significantly enhanced by its N-terminal truncation. In contrast, Trp58 and Trp85 had little influence. The N-terminal successive truncations of Scb and its mutants resulted in the weaken inhibitors to papain. These results suggested that the N-terminal region of Scb interacts with the peptide segment preceding the first hairpin loop, thereby stabilizing the conformation of the hairpin loop structure.

K. Doi-Kawano · Y. Kouzuma · M. Kimura
Laboratory of Biochemistry,
Department of Bioscience and Biotechnology,
Faculty of Agriculture, Graduate School of Kyushu University,
Hakozaki,
Fukuoka 812-8581, Japan

E. Nishimoto · D. Takahashi · S. Yamashita (✉)
Institute of Biophysics,
Department of Bioscience and Biotechnology,
Faculty of Agriculture, Graduate School of Kyushu University,
Hakozaki,
Fukuoka 812-8581, Japan
e-mail: yamashita@brs.kyushu-u.ac.jp

Keywords Proteinase inhibitor · Cystatin · Time-resolved fluorescence · Fluorescence depolarization · Single Trp protein

Abbreviations

rScb	recombinant sunflower cystatin b
Sca	sunflower cystatin a
W85F/T52W	recombinant sunflower cystatin b of which Trp85 and Thr52 are replaced with Phe and Trp, respectively
W85F/T58W	recombinant sunflower cystatin b of which Trp85 and Thr58 are replaced with Phe and Trp, respectively

Introduction

Cysteine protease inhibitors belonging to the cystatin superfamily have been found in several plant tissues, such as seeds, tubers, and ripening fruits; they are referred to as phytocystatin [1]. Phytocystatins are single polypeptide chains with molecular weight from 10–12 kDa and share three conserved sequence motifs: Gly in the vicinity of the N-terminal region, Gln-Xaa-Val-Xaa-Gly in the first hairpin loop, and Trp in the second loop [1]. Recently, the three-dimensional structure of oryzacystatin from rice seeds has been determinated by NMR, and showed that the structure is highly homologous to those of mammal cystatins [2].

The nature of the interaction of cystatin and protease has been extensively studied on mammal cystatins [3, 4]. The X-ray structure analysis of chicken cystatin showed that N-terminal segment and two hairpin loops are exposed on the surface of the protein, forming a wedge shaped edge [5]. Docking model suggested that this wedge fits into the

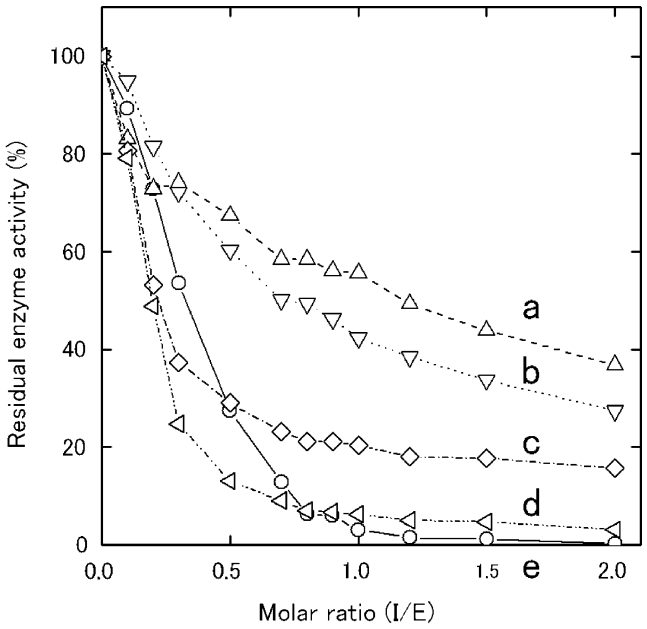

Fig. 1 Inhibitory activities of rScb and its mutants. The relative residual activity of papain was plotted against the molar ratio (I/E) of the inhibitor to papain. **a** W85; **b** W85A; **c** W85H; **d** W85F; **e** rScb

active site cleft of papain [5]. This assumption was confirmed by structure analysis of cystatin B in complex with papain [6]. In this structure, a wedge formed by the N-terminal end and two hairpin loops of cystatin B fits well into the active site cleft of papain. Although the functional implication of the first and second hairpin loops in the inhibitory activity was demonstrated by biochemical studies [7, 8], the contribution of the N-terminal region was controversial for some cystatins. Cystatin B derivative, in which 6 N-terminal amino acid residues including Gly were missing, was found to exhibit inhibitory activity, indicating that the N-terminal region is dispensable for inhibition [9]. Pol and Björk described that mutation of Cys3 by Ser in human cystatin B caused reduced inhibitory activity, indicating the importance of the N-terminal region of the cystatin B [10]. Furthermore, the N-terminal truncation of oryzacystatin had little effect on the inhibitory activity, suggesting that the N-terminal region is not involved in inhibitory activity [11]. By contrast, subsequent mutagenesis study showed indispensability of the N-terminal region of oryzacystatin [12].

On the other hand, the implication of the N-terminal regions of cystatin A, cystatin C, and chicken cystatin in the inhibitory activity were well demonstrated by extensive biochemical studies [13–17]. It was recently described by kinetic study that cystatin A inhibits cysteine proteinases in two steps: the N-terminal region inhibits proteinases subsequent to other hairpin loops, and proposed that independent binding of the N-terminal region of cystatins to target proteinases after hairpin loops may be characteristic of most cystatin-proteinase interactions [18]. In addition, Shibuya et al. found by NMR spectroscopic analysis of cystatin A that the mutation of the Gly4 residue caused chemical shifts of the Gln-Val-Val-Ala-Gly sequence, suggesting that the N-terminal region may be not only involved in direct interaction with proteinases, but also in maintaining the conformation of the first hairpin loop [19].

In our own study, two phytocystatins designated Sca and Scb were isolated from sunflower (*Helianthus annuus*) seeds. Sca and Scb consist of 80 and 98 amino acid residues, respectively, and exhibit inhibitory activity toward papain and fitin [20]. Scb is a basic protein with the pI value of 10, and extra 5 amino acids in the middle of the molecule. The successive truncation of the N-terminal residues of Scb resulted in decreased inhibitory activity toward papain [21]. These findings suggested that Scb inhibits proteinase in the manner similar to those of mammal cystatins. Fluorescence spectroscopy is an excellent method to study the correlation between the structure and function of protein. Especially, the time-resolved method with high sensitivity and time-resolution power enable to detect and analyze delicate but essential conformation and dynamics for the protein functions through the tryptophan residue of which location is specified in 3D structure of proteins. In this study, the interaction of the N-terminal region with the first and second hairpin loops was investigated using the steady-state and time-resolved fluorescence spectroscopic measurements of the recombinant Scb (rScb) and its mutant proteins. The results suggested that

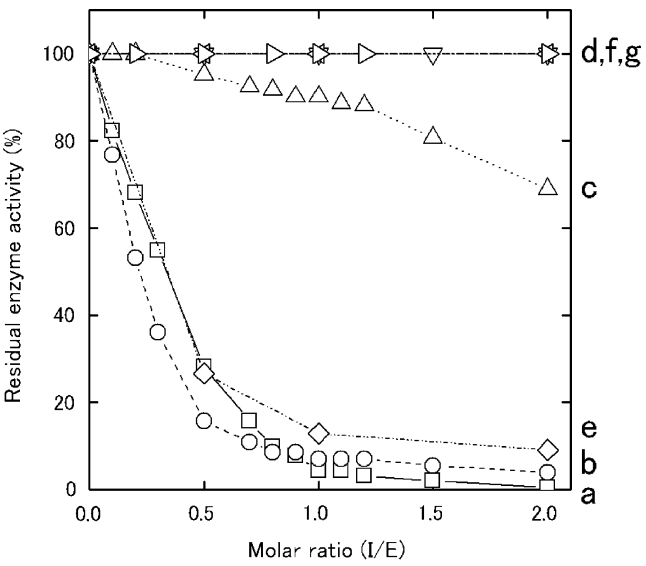

Fig. 2 Inhibitory activities of rScb and its mutants. The relative residual activity of papain was plotted against the molar ratio (I/E) of the inhibitor to the enzyme. **a** rScb; **b** W85F/T52W; **c** W85F/T52W/N1; **d** W85F/T52W/N4; **e** W85F/T58W; **f** W85F/T58W/N1; **g** W85F/T58W/N4

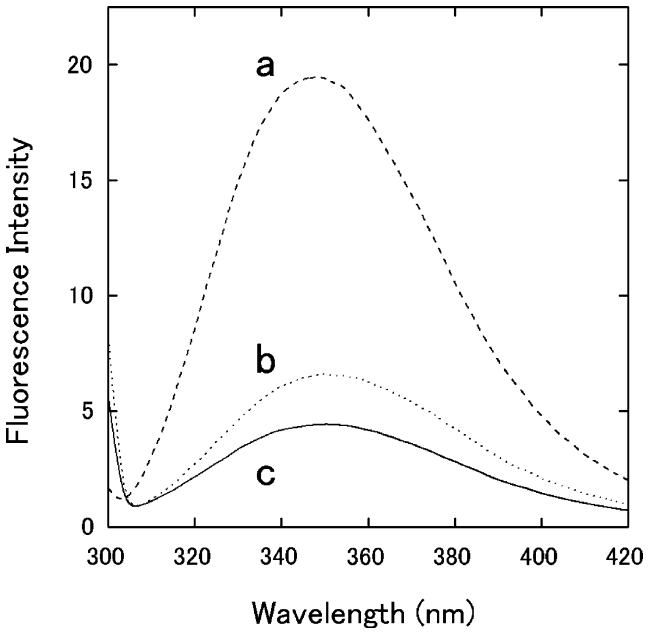

Fig. 3 Fluorescence spectra of W85F/T52W (**a**), W85F/T58W (**b**), and rScb (**c**). Excitation wavelength, 300 nm. The concentration of a, b, and c were adjusted to be OD_{280}=0.1

the N-terminal region plays an essential role in stabilizing the conformation of the first hairpin loop structure within Scb.

Materials and methods

Materials Restriction enzymes and DNA modifying enzymes were purchased from MBI Fermentas and Toyobo, respectively. The oligonucleotide primers used in this study and thermo sequenase cycle sequencing kit containing 7-deaza-dGTP were obtained from GE Healthcare Bio-Science Corp. A chameleon double standard site-directed mutagenesis kit was from Strategene. Plasmid pGEM T-vector and expression plasmid pET-22b were obtained from Promega and Novagen, respectively. *Escherichia coli* strains JM109 and XlmutS were used as host cells for cloning and mutagenesis, and the strain BL21(DE3) was used as host cells for producing the recombinant Scb (rScb) as well as its mutant proteins. All other common chemicals and reagents were purchased at the highest purity available.

Mutagensis and DNA sequencing For mutagenesis experiments, the cDNA coding for Scb in the plasmid pGEM T-vector was used. Site-directed mutagenesis was performed by the unique site elimination method developed by Deng and Nickoloff [22]. All the mutations introduced were confirmed by DNA sequencing with a DNA sequencer (Shimadzu, DSQ-1000) using a thermo sequenase cycle sequencing kit (GE Healthcare Bio-Science Corp.).

Expression and purification of the recombinant proteins The genes encoding wild-type and mutant Scb were expressed in *E. coli* strain BL21(DE3) using the expression plasmid pET-22b [23], as described in ref. 21. Proteins were purified from total extracts of the cells as previously described. The purity of wild-type and mutant enzymes was confirmed by reversed phase HPLC on a Cosmosil 5C4-300 (4.6×150 mm) and SDS-PAGE using 15% polyacrylamide gel. Deletions at the N-terminal residues were verified by N-terminal amino acid sequence using a gas-phase protein sequencer (Shimadzu, PSQ-1). Proteinase inhibitory assays were done, as previously described using the substrate Pyr-Phe-Leu p-nitrosoanilide [20]. Concentration of rScb and its mutants were adjusted spectrophotometrically.

Steady state fluorescence Every phytocystatin was prepared in 10 mM Na-phosphate buffer (pH 7.0). Steady-state fluorescence emission spectra were measured on Hitachi 850 fluorescence spectrophotometer. Each emission spectrum was strictly corrected for the excitation-detection response of the instrument and for the stray light.

Table 1 Fluorescence decay parameters at 350 nm of cystatins [a]

	τ_1	τ_2	τ_3	α_1	α_2	α_3	F_1 [b]	F_2	F_3	τ_{av} [c]
rScb	3.25	1.08	0.29	0.12	0.45	0.43	0.40	0.47	0.13	0.98
rScb/N2[d]	3.17	1.04	0.32	0.14	0.44	0.42	0.43	0.45	0.12	1.03
rScb/N4	3.02	0.95	0.28	0.13	0.46	0.41	0.42	0.46	0.12	0.94
W85F/T52W	4.28	1.50	0.10	0.59	0.21	0.19	0.88	0.11	0.01	2.27
W85F/T52W/N2	4.03	1.47	0.09	0.70	0.15	0.16	0.93	0.07	0.00	3.04
W85F/T52W/N4	4.07	1.44	–	0.90	0.10	–	0.96	0.04	–	3.80
W85F/T58W	3.88	1.40	0.26	0.15	0.54	0.31	0.41	0.54	0.05	1.42
W85F/T58W/N2	3.22	1.26	0.21	0.16	0.59	0.25	0.39	0.57	0.04	1.31
W85F/T58W/N4	3.26	1.30	0.22	0.15	0.60	0.24	0.37	0.59	0.04	1.32

[a] Excitation wavelength, 300 nm; emission wavelength, 350 nm.
[b] $F_i = \alpha_i\tau_i / \sum \alpha_i\tau_i$.
[c] $\tau_{av} = \sum \alpha_i\tau_i$.
[d] N2 and N4 indicate N-terminal 2 and 4 amino acid residues deleted mutants, respectively.

Time-resolved fluorescence and fluorescence anisotropy studies The fluorescence decay measurements were performed using the pico-second laser/multichannel plate based time-correlated single photon counting technique. The excitation source was a frequency-doubled output from cavity-dumped dye laser. The excitation pulse was a strain of 11 ps wide pulses wit a repetition rate of 800 kHz. The excitation wavelength was 300 nm, and the emission was detected after passing through a monochromator (H10, Jobin Yvon) with a 4 nm bandpass onto a multichannel plate photomultiplier tube (R1564, Hamamatsu). The channel width of the multichannel analyzer was 10 ps, and the data was collected in 2048 channels. The instrumentation used here was described elsewhere [24]. Fluorescence decay data were analyzed by a nonlinear least squares iterative convolution method based on the Marquardt algorithm [25]. Adequacy of the fitting was judged by inspection of the weighted residuals and of statistical parameters such as sigma and the serial variance ratio (SVR). For a satisfactory fit, the weighted residual must be randomly distributed and sigma and SVR should be in ranges of 1.0–1.2 and 1.8–2.0, respectively.

The fluorescence anisotropy decay measurement was performed by using the same instrument as fluorescence decay measurement. But, the parallel and perpendicular components were measured separately by orienting Glan-Taylor polarizers vertically and horizontally against the vertical excitation. The G-factor in the wavelength region

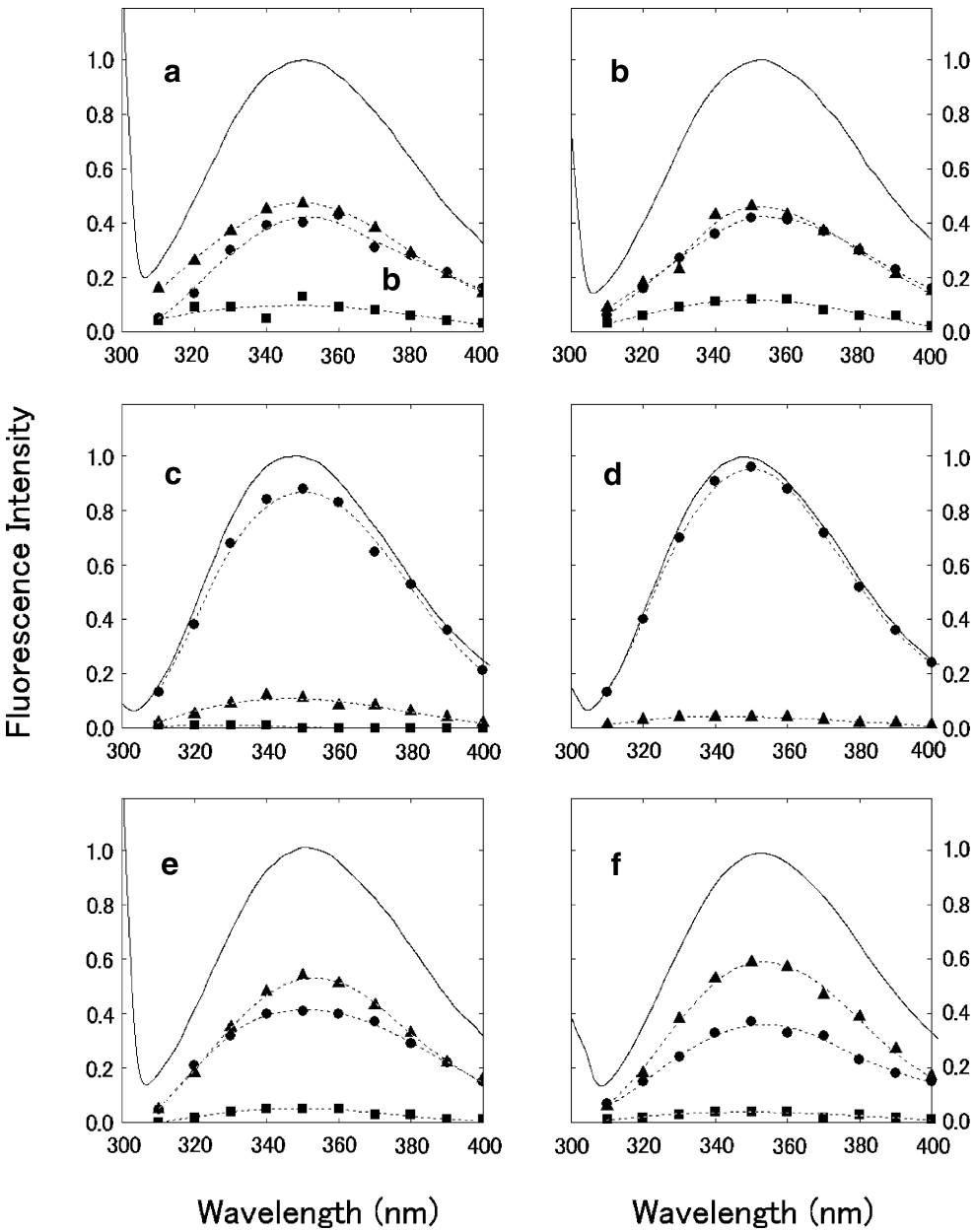

Fig. 4 Decay associated spectra of rScb and its mutants. **a**, **c**, and **e** are rScb, W85F/T52W, and W85F/T58W, respectively, and **b**, **d**, and **f** were their N-terminal 4 amino acids deleted mutant, respectively

300–400 nm was determined by using azanaphthen in ethanol as an isotropic fluorescence standard. Adequacy of the fluorescence anisotropy decay was judged by the nonlinear least square curve fitting based on the Marquardt-Levenberg algorithm [26].

Results and discussion

Preparation and characterization of mutant proteins

Fluorescence spectroscopic studies using Trp as a fluorescence probe provide useful insight into the motion and interactions between the peptide elements of protein. Especially, specified the location of fluorophore in protein, the time-resolved study can provide the more quantitative information. Scb contains one Trp85 at the second loop structure. To probe the interaction of the N-terminal region with the first (positions 53–57: QVVAG) and second (positions 84–87: SWKH) loops by fluorescence spectroscopy, Trp was introduced around the first loop. For this purpose, Trp85 was first replaced with other amino acids or deleted, and the resulting mutants were characterized in term of the inhibitory activity.

Four Scb mutants in which Trp85 was either replaced with Ala, His, and Phe, or deleted, were overproduced in *E. coli* BL21 (DE3) using the T7 system as described previously [21]; the resulting mutants were referred to as W85A, W85H, W85F, and desW85, respectively. All mutant proteins were purified from the inclusion bodies, as described for rScb, so as to give a single band on SDS-PAGE. Inhibitory potency of these mutant proteins toward papain were assayed using Pyr-Phe-Leu p-nitrosoanilide as substrate. As shown in Fig. 1, the mutant W85F retained the inhibitory activity of the same extent as wild-type, while other three mutants showed lower inhibitory activities. Hence, the mutant W85F was used for generation of Trp-induced mutant proteins.

The Trp-introduced mutants W85F/T52W, W85F/V54W, W85F/V55W, and W85F/T58W, in which the amino acids Thr52, Val54, Val55, and Thr58 around the first loop were in turn replaced with Trp, were generated, and the resulting mutants were overproduced and characterized in term of inhibitory activity toward papain. The result showed that mutation of Thr52 and Thr58 had no effect on the inhibitory activity, whereas those of Val54 and Val55 caused significant decreased inhibitory activity. Therefore, two mutants W85F/T52W and W85F/T58W were used for generation of the successive N-terminal truncated mutants. The N-terminal successive truncations of Scb mutants progressively reduced their activity as shown in Fig. 2. Four residues truncation made all three Scb mutants almost inactive.

Steady state and time-resolved fluorescence studies

When rScb, W85F/T52W, and W85F/T58W are excited at 300 nm, the fluorescence spectra due to W85, W52, and W58 are observed, respectively. They showed the fluorescence maxima at 352, 346, and 350 nm, respectively, to suggest that the tryptophan residues of three phytocystatins locate at the protein surface although W52 is in less polar circumstance (Fig. 3). The fluorescence of W85F/T52W showed much higher intensity than other two cystatins, rScb, and W85F/T58W. Only the fluorescence intensity of W85F/T52W was increased when the N-terminal deleting effects on the fluorescence spectra of the wild and mutant cystatin were examined. by the deleting of N-terminal amino acids.

The fluorescence decay kinetics of the phytocystatins gave the fit to the linear combination of triple-exponentials regardless the location of the tryptophan residue. Three components were characterized with each decay time, the longer (τ_1), medium (τ_2), and shorter (τ_3), respectively. As shown in Table 1, the decay kinetics of rScb and W85F/T58W were not so much affected by removing the N-terminal amino acids although every three decay times became shorter and therefore, the average lifetime became shorter. But W85F/T52W reduced the fastest decay component to change its decay kinetics from the triple exponential to double. The shortest decay time of W85F/T52W was about 100 ps and it was extraordinarily shorter than that of the other cystatins. These facts demonstrate that some specific amino acid residue such as N-terminal amino acid, lysine or glutamate which has the charged amino or uncharged carboxyl group approaches to Trp52 to quench the fluorescence of tryptophan residue. Trp52 was free from the interaction with those residues by removing the N-terminal amino acids shown by that the average lifetime was increased.

Table 2 The relative concentration of ground state Trp conformers of cystatins

	C_1[a]	C_2	C_3
rScb	0.12	0.45	0.42
rScb/N1[b]	0.11	0.41	0.48
rScb/N2	0.14	0.46	0.40
rScb/N4	0.16	0.49	0.35
W85F/T52W	0.59	0.21	0.20
W85F/T52W/N1	0.62	0.16	0.22
W85F/T52W/N2	0.63	0.15	0.20
W85F/T52W/N4	0.89	0.11	0
W85F/T58W	0.16	0.51	0.34
W85F/T58W/N1	0.16	0.51	0.33
W85F/T58W/N2	0.16	0.52	0.32
W85F/T58W/N4	0.15	0.58	0.27

[a] $C_i = (A_i/\tau_i)\sum A_i/\tau_i$. (See text.)
[b] N1, N2 and N4 indicate N-terminal 1, 2 and 4 amino acid residues deleted mutants, respectively.

The global analysis covering the entire spectral region demonstrated that the decay times in the fluorescence decay kinetics of each phytocystatin were independent on the emission wavelength. Therefore, the decay-associated spectrum (DAS) of every cystatin is given by

$$I_i(\lambda) = I_{ss}(\lambda)\left[\alpha(\lambda)\tau_i \Big/ \sum \alpha_i(\lambda)\tau_i\right] \quad (1)$$

where $I_{ss}(\lambda)$ is the steady state fluorescence spectrum and τ_i and $\alpha_i(\lambda)$ are the i-th decay time and the corresponding pre-exponential factor in the decay kinetics, respectively. As shown in Fig. 4, DAS of rScb and W85F/T58W were not affected so much by the removing the N-terminal amino acids. In the DAS of W85F/T52W, more than 80% was occupied by the longer decay component and the fractions of the other two components were very small. But the trace of the fastest decay component was clearly recognized. According to Willis et al., the relative concentration of the ground state conformer (C_i) which is the origin of the component in the DAS is given by the decay time and the integrated area of i-th component (A_i). [27]

$$C_i = (A_i/\tau_i)\left(\sum A_i/\tau_i\right) \quad (2)$$

The estimated concentrations of the ground state conformers of every phytocystatins investigated here were summarized in Table 2. It should be noted that the fraction of

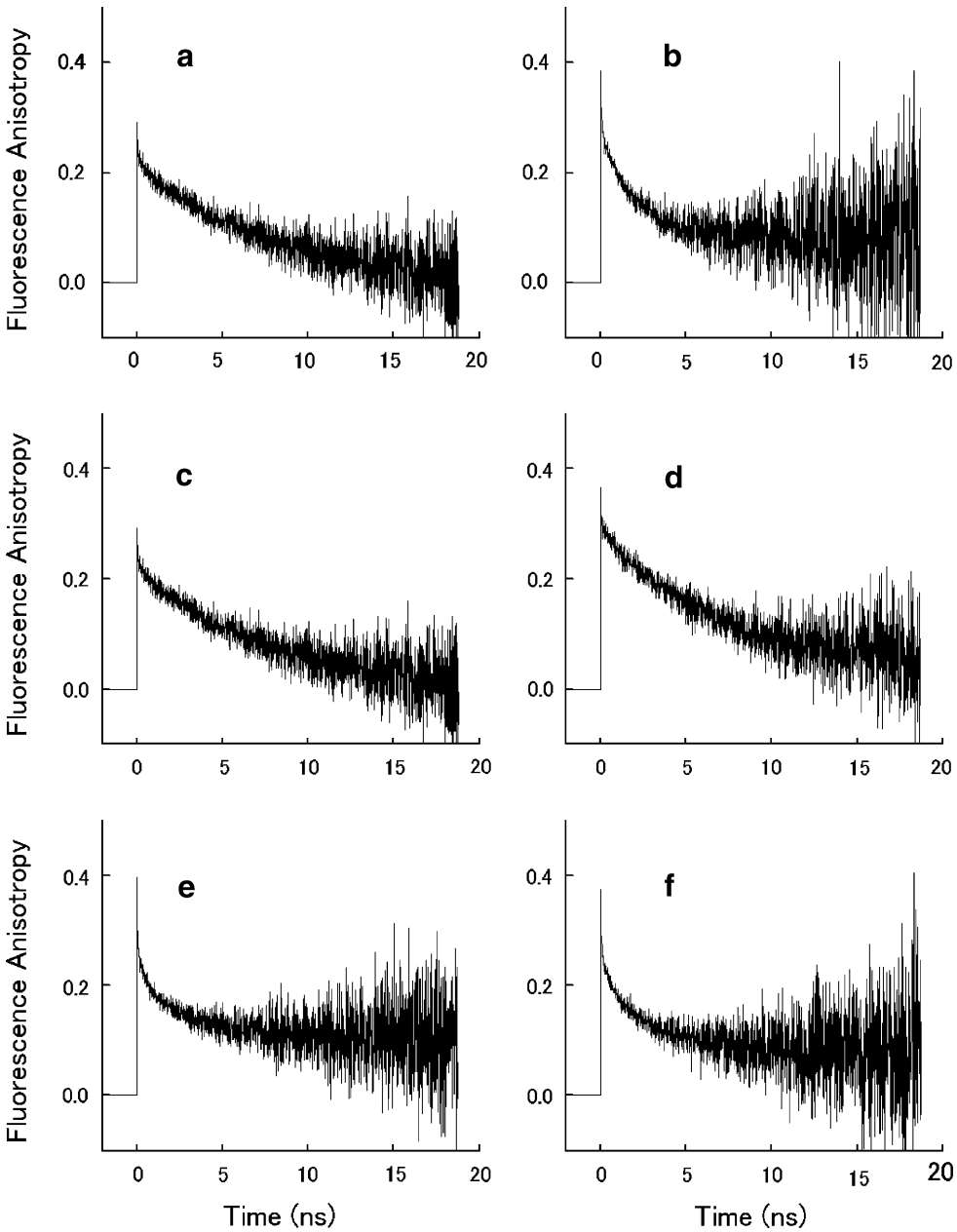

Fig. 5 Fluorescence anisotropy decay of rScb and its mutants. Excitation and emittion wavelength were 300 nm and 350 nm, respectively. **a** rScb; **b** rScb/N4; **c** W85F/T52W; **d** W85F/T52W/N4; **e** W85F/T58W; **f** W85F/T58W/N4

Table 3 Fluorescence anisotropy decay parameters of cystatins [a]

	β_1	β_2	β_3	φ_1(ps)	φ_2(ns)	φ_3(ns)	f	θ (°)
rScb	0.20	0.13	0.11	20	1.27	9.62	0.75	52
rScb/N2[b]	0.18	0.17	0.08	140	2.54	9.00	0.81	56
rScb/N4	0.18	0.17	0.07	140	2.50	8.97	0.83	58
W85F/T52W	0.08	0.03	0.25	67	2.43	11.0	0.30	28
W85F/T52W/N2	0.07	0.06	0.22	90	3.03	9.08	0.37	31
W85F/T52W/N4	0.10	0.07	0.22	<10	3.85	7.95	0.44	35
W85F/T58W	0.17	0.11	0.10	270	2.95	9.62	0.74	51
W85F/T58W/N2	0.17	0.13	0.09	360	2.07	9.01	0.77	53
W85F/T58W/N4	0.19	0.13	0.08	440	3.24	9.00	0.78	54

[a] Excitation wavelength, 300 nm; emission wavelength, 350 nm.
[b] N2 and N4 indicate N-terminal 2 and 4 amino acid residues deleted mutants, respectively.

the conformer of W85F/T52W giving the shortest decay time was 20% and was not found in W85F/T52W of which N-terminal 4 amino acids were removed. The conformers giving the faster decay time in W85F/T58W and rScb also decreased about 30% by removing the N-terminal amino acids.

The time-resolved fluorescence depolarization analysis of the recombinant and mutant cystatin supported that Trp52 would be under the specific influence of the N-terminal residue from the standpoint of the molecular dynamics. The fluorescence anisotropy decay curves of rScb, W85F/T52W, W85F/T58W and their N-terminal removed mutants are shown in Fig. 5. When these decay curves were described with three components characterized by the rotational correlation times (ϕ_i) and the corresponding amplitudes (β_i), respectively.

$$r(t) = \sum \beta_i \exp(-t/\phi_i) \tag{3}$$

The kinetic parameters are summarized in Table 3. Since the longest correlation times (ϕ_3) were in the time range of 8–10 ns, they would be due to the entire rotation of the cystatin. The correlation time of the protein with molecular weight of 10 kDa is estimated to be about 9 ns by using the viscosity, 1.0 cp, hydration, 0.4 and partial specific volume, 0.73 ml/mg based on the Einstein-Stokes law [28]. By removing a few N-terminal amino acid residues, the longest correlation times were reduced. The other two components are presumably due to the depolarization by the rotational motions of the peptide segment including Trp residue and the fast fluctuation of the Trp residue itself, respectively. Assuming every motions depolarize the fluorescence are independent each other, the motional freedom of these motion (f_i) was connected with the amplitude in the fluorescence anisotropy decay kinetics

$$f_i = \beta_i \Big/ \sum \beta_i \tag{4}$$

The motional freedom of tryptophan residue in each cystatin was shown in Table 3. By removing the N-terminal 4 amino acids, the freedom of the segmental motions of Trp85 and Trp58 in rScb and W85F/T58W increased a little, 5–10%. The motional freedom of rapid fluctuation of Trp52 in W85F/T52W-cystatin was smaller. But, it was increased more than 150% by removing the N-terminal 4 amino acids suggesting that the segmental motion of the peptide chain around Trp52 was much enhanced. The fastest correlation time dropped down to below 10 ps by the removing N-terminal 4 amino acids. These results reveal that the N-terminal amino acids do not only contribute to the packing structure in the local areas around Trp85 and

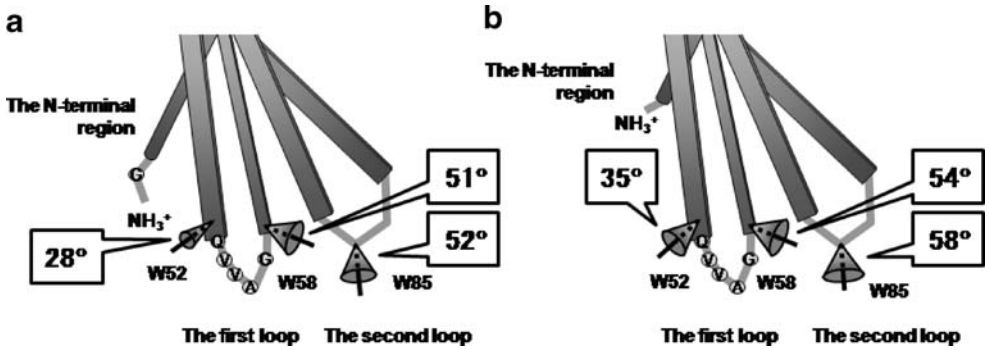

Fig. 6 The effect of the N-terminal amino acid deletion on the segmental motion of Trp residue. **a** cystatin; **b** N-terminal amino acid deleted cystatin. The backbone structure was based on the chicken cystatin

Trp58 but also control the free fluctuation of the peptide chain by interacting with Trp52.

W85F/T52W and W85F/T58W exhibited the same inhibitory activities against the proteinase as rScb. Therefore, it is reasonable to consider that they reserved the essential structure for completing their function. At the same time, the elimination of the N-terminal amino acid residues similarly reduced their inhibitory activities. This fact demonstrates that the N-terminal residue plays an essential role for the inhibitory activity against the proteinase.

The time-resolved fluorescence studies on the rScb and other mutant phytocystatins used here consistently showed the N-terminal residue would approach and interact with Trp52. First of all, Trp52 in W85F/T52W showed very fast decay time in the order of 100 ps. This suggests that there exist the stronger fluorescence quenching side chain around Trp52. The strongest fluorescence quenching side chain is disulfide linkage which quenches the tryptophyl fluorescence through the electron exchange interaction. But its interaction is limited within the very short range. Other protonated amino group and deprotonated carboxylic group quench the tryptophyl fluorescence through the proton and electron transfer in the excited state, respectively. According to the anticipated X-ray crystallographic structure of Scb, there is no amino group and carboxylic group to quench the tryptophyl fluorescence around Thr52. Therefore, the N-terminal amino group must be approaching to Trp52 and one of the three conformers would strongly interact with N-terminal amino group. Because the DAS fraction corresponding to the fastest decay time was not recognized in the mutant of W85F/T52W of which N-terminal 4 amino acids were eliminated.

The fluorescence anisotropy decay analysis of rScb and its mutant phytocystatins also supported that the N-terminal amino acid interacts with the residues locate at the first loop of Scb. Using the order parameter (S^2) and the motional freedom obtained in the fluorescence anisotropy measurements, the segmental motion of the tryptophan residue can be expressed with the semi-cone angle (θ) [29, 30].

$$S^2 = 1 - \sum f_i = \left(\frac{1}{2}\cos\theta(\cos\theta + 1)\right)^2 \quad (5)$$

The semi-cone angles of motional freedom of Trp85, Trp52, and Trp58 of rScb, W85F/T52W, and W85F/T58W are changed from 52°–58°, 28°–35° and 51°–54° by eliminating N-terminal 4 amino acids, respectively. These results were schematically shown in Fig. 6. It is clear that the segmental motion of Trp52 is free from the suppressive interaction with the N-terminal amino acid.

Shibuya et al. indicated the relevance of the N-terminal amino acid in the inhibitory activity by the chemical shift in NMR induced at the hairpin loop [14]. The time-resolved fluorescence study using the single Trp mutant phytocystatin are consistent with their observations and showed that N-terminal amino acid would be under the interaction with the vicinity of Thr52 to stabilize the conformation of the first hairpin loop. Presumably, it would be one of the essential factors for Scb to complete the inhibitory activity against the proteinase.

References

1. Kondo H, Abe K, Nishimura I, Watanabe H, Emori Y, Arai S (1990) Two distinct cystatin species in rice seeds with different specificities against cysteine proteinases. Molecular cloning, expression, and biochemical studies on oryzacystatin-II. J Biol Chem 265:15832–15837
2. Nagata K, Kudo N, Abe K, Arai S, Tanokura M (2000) Three-dimensional solution structure of oryzacystatin-I, a cysteine proteinase inhibitor of the rice, *Oryza sativa* L. japonica. Biochemistry 39:14753–14760
3. Barrett AJ, Rawlings ND, Davies ME, Machleidt W, Salvesen G, Turk V (1986) In Proteinase Inhibitors. Elsevier, Amsterdam, pp 515–569
4. Turk B, Turk V, Turk D (1997) Structural and functional aspects of papain-like cysteine proteinases and their protein inhibitors. Biol Chem 378:141–150
5. Bode W, Enbh R, Musil D, Thiele U, Huber R, Karshikov A, Brzin J, Kos J, Turk V (1988) The 2.0 A X-ray crystal structure of chicken egg white cystatin and its possible mode of interaction with cysteine proteinases. EMBO J 7:1939–1947
6. Stubbs MT, Laber B, Bode W, Huber R, Jerala R, Lenarcic B, Turk V (1990) The refined 2.4 A X-ray crystal structure of recombinant human stefin B in complex with the cysteine proteinase papain: a novel type of proteinase inhibitor interaction. EMBO J 9:1939–1947
7. Pol E, Björk I (1999) Importance of the second binding loop and the C-terminal end of cystatin B (stefin B) for inhibition of cysteine proteinases. Biochemistry 38:10519–10526
8. Björk I, Brieditis I, Raub-Segall E, Pol E, Hakansson K, Abrahamson M (1996) The importance of the second hairpin loop of cystatin C for proteinase binding. Characterization of the interaction of Trp-106 variants of the inhibitor with cysteine proteinases. Biochemistry 35:10720–10726
9. Thiele U, Assfalg-machleidt I, Machleidt W, Auerswald EA (1990) N-terminal variants of recombinant stefin B: effect on affinity for papain and cathepsin B. Biol Chem Hopper-Seyler 371 (Suppl.):125–136
10. Pol E, Björk I (2001) Role of the single cysteine residue, Cys 3, of human and bovine cystatin B (stefin B) in the inhibition of cysteine proteinases. Protein Sci 10:1729–1738
11. Abe K, Emori Y, Kondo H, Arai S, Suzuki K (1988) The NH_2-terminal 21 amino acid residues are not essential for the papain-inhibitory activity of oryzacystatin, a member of the cystatin superfamily. Expression of oryzacystatin cDNA and its truncated fragments in Escherichia coli. J Biol Chem 263:7655–7659
12. Urwin PE, Atkinson HJ, Mcpherson MJ (1995) Involvement of the NH2-terminal region of oryzacystatin-I in cysteine proteinase inhibition. Protein Eng 8:1303–1307
13. Estrada S, Pavlova A, Björk I (1999) The contribution of N-terminal region residues of cystatin A (stefin A) to the affinity and kinetics of inhibition of papain, cathepsin B, and cathepsin L. Biochemistry 38:7339–7345

14. Shibuya K, Kaji H, Ohyama Y, Tate S, Kainosho M, Inagaki F, Samejima T (1995) Significance of the highly conserved Gly-4 residue in human cystatin A. J Biochem 118:635–642
15. Hall A, Hakansson K, Mason RW, Grubb A, Abrahamson M (1995) Structural basis for the biological specificity of cystatin C. Identification of Leu-9 in the N-terminal binding region as a selectivity-conferring residue in the inhibition of mammalian cysteine peptidases. J Biol Chem 270:5115–5121
16. Mason RW, Sol-Church K, Abrahamson M (1998) Amino acid substitutions in the N-terminal segment of cystatin C create selective protein inhibitors of lysosomal cysteine proteinases. Biochem J 330:833–838
17. Lindahl P, Ripoll D, Abrahamson M, Mort JS, Storer AC (1994) Evidence for the interaction of valine-10 in cystatin C with the S2 subsite of cathepsin B. Biochemistry 33:4384–4392
18. Estrada S, Olson ST, Raub-Segall E, Björk I (2000) The N-terminal region of cystatin A (stefin A) binds to papain subsequent to the two hairpin loops of the inhibitor. Demonstration of two-step binding by rapid-kinetic studies of cystatin A labeled at the N-terminus with a fluorescent reporter group. Protein Sci 9:2218–2224
19. Shubuya K, Kaji H, Itoh T, Ohyama Y, Tsujukami A, Tate S, Takeda A, Kumagai I, Hirao I, Miura K, Inagaki F, Samejima T (1995) Human cystatin A is inactivated by engineered truncation. The NH_2-terminal region of the cysteine proteinase inhibitor is essential for expression of its inhibitory activity. Biochemistry 34:12185–12192
20. Kouzuma Y, Kawano K, Kimura M, Yamasaki N, Kadowaki T, Yamamoto K (1996) Purification, characterization, and sequencing of two cysteine proteinase inhibitors, Sca and Scb, from sunflower (*Helianthus annuus*) seeds. J Biochem 119:1106–1113
21. Doi-Kawano K, Kouzuma Y, Yamasaki N, Kimura M (1998) Molecular cloning, functional expression, and mutagenesis of cDNA encoding a cysteine proteinase inhibitor from sunflower seeds. J Biochem 124:911–916
22. Deng WP, Nickoloff JA (1992) Site-directed mutagenesis of virtually any plasmid by eliminating a unique site. Anal Biochem 200:81–88
23. Studier FW, Rosenberg AH, Dunn JJ, Dubendorff JW (1990) Use of T7 RNA polymerase to direct expression of cloned genes. Methods Enzymol 185:60–89
24. Yamashita S, Nishimoto E, Szabo AG, Yamasaki N (1996) Steady-state and time-resolved fluorescence studies on the ligand-induced conformational change in an active lysozyme derivative, Kyn62-lysozyme. Biochemistry 35:531–537
25. McKinnon AE, Szabo AG, Miller DR (1977) The deconvolution of photoluminescence data. J Phys Chem 81:1564–1570
26. Gill PR, Murray W, Wright MH (1981) The Levenberg-Marquardt method. Practical optimization. Academic Press, London, pp 136–137
27. Willis KJ, Szabo AG (1992) Conformation of parathyroid hormone: time-resolved fluorescence studies. Biochemistry 31:8924–8931
28. Lakowicz JR (1999) Principles of fluorescence spectroscopy, 2ndnd edn. Kluwer Academic/Plenum, New York
29. Lipari G, Szabo A (1982) Model-free approach to the interpretation of nuclear magnetic resonance relaxation in macromolecules. 2. Analysis of experimental results. J Am Chem Soc 104:4559–4570
30. Nishimoto E, Yamashita S, Szabo AG, Imoto T (1998) Internal motion of lysozyme studied by time-resolved fluorescence depolarization of tryptophan residues. Biochemistry 37:5599–5607